Nitric oxide protects against ferroptosis by aborting the lipid peroxidation chain reaction

Takujiro Homma[1,*], Sho Kobayashi[1], Marcus Conrad[2], Hiroyuki Konno[3], Chikako Yokoyama[4], and Junichi Fujii[1]

[1] Department of Biochemistry and Molecular Biology, Graduate School of Medical Science, Yamagata University, 2-2-2 Iidanishi, Yamagata 990-9585, Japan

[2] Helmholtz Zentrum München, Institute of Metabolism and Cell Death, Ingolstädter Landstr. 1, 85764, Neuherberg, Germany

[3] Department of Biological Engineering, Graduate School of Science and Engineering, Yamagata University, Yonezawa, Yamagata, 992-8510, Japan

[4] Department of Applied Chemistry and Bioengineering, Graduate School of Engineering, Osaka City University, 3-3-138, Sugimoto, Sumiyoshi-ku, Osaka-shi, 558-8585, Japan

*Correspondence author: Takujiro Homma

17 e-mail: tkhomma@med.id.yamagata-u.ac.jp

18 Tel. +81-23-628-5229; Fax +81-23-628-5230

Abstract

Ferroptosis is a type of iron-dependent necrotic cell death, which is typically triggered by the depletion of intracellular glutathione (GSH), which is associated with increased lipid peroxidation. Nitric oxide (NO) is a highly reactive gaseous radical mediator with anti-oxidation properties that terminates lipid peroxidation reactions. In the current study, we report the anti-ferroptotic action of NOC18, an NO donor that spontaneously releases NO, in cells under various ferroptototic conditions in vitro. Our results indicate that, when mouse hepatoma Hepa 1-6 cells are incubated with NOC18, cell death induced by various ferroptotic stimuli such as cysteine (Cys) starvation, the inhibition of glutathione peroxidase 4 (GPX4) and treatment with tertiary-butyl hydroperoxide (TBHP) is significantly reduced. Treatment with NOC18 failed to improve the decrease in the levels of Cys or GSH and the accumulation of ferrous iron upon ferroptotic stimuli. The fluorescent intensity of C11-BODIPY$^{581/591}$, a probe that is used to detect lipid peroxidation products, was increased somewhat by treatment with NOC18 under conditions of Cys starvation, the accumulation of lipid peroxidation end-products, as evidenced by the levels of 4-hydroxynonenal, were effectively

suppressed. The pre-incubation of TBHP with NOC7, a short-lived NO donor completely eliminated its ability to trigger ferroptosis. These collective results indicate that NO exerts a cytoprotective action against various ferroptotic stimuli by aborting the lipid peroxidation chain reaction.

Key words

ferroptosis; glutathione; lipid peroxidation; nitric oxide; ROS

Abbreviations

Cys: cysteine

GSH: glutathione

GPX4: phospholipid hydroperoxide-glutathione peroxidase

LC-MS: liquid chromatography-mass spectrometry

LDH: lactate dehydrogenase

NO: nitric oxide

PI: propidium iodide

ROS: reactive oxygen species

TBHP: tertiary-butyl hydroperoxide

1. Introduction

Ferroptosis is a type of iron-dependent, regulated cell death that occurs as a consequence of lipid peroxidation [1,2]. The reduction of ferric iron (Fe^{3+}) to ferrous iron (Fe^{2+}) in the presence of peroxides triggers the production of hydroxyl radicals generally through Fenton-type reactions [3], leading to the initiation of lipid peroxidation. The resulting lipid peroxides that are generated in membrane phospholipids cause ferroptotic cell death by disrupting the integrity of the plasma membrane. Glutathione (GSH), a cysteine (Cys)-centered tripeptidyl redox molecule, plays a pivotal role in protecting against the accelerated lipid peroxidation associated with ferroptosis. The anti-ferroptotic action of GSH can be largely attributed to glutathione peroxidase 4 (GPX4), which reductively detoxifies lipid peroxides by utilizing GSH as an electron donor in the ferroptotic process [4]. xCT, the core transporter protein of system x_c^-, is responsible for the cellular uptake of cystine, an oxidized Cys dimer linked by a disulfide bridge [5]. Because the availability of free Cys is the major determinant of GSH synthesis, ferroptosis can be readily induced by either Cys starvation (e.g. the deprivation of cystine from the culture medium or the inhibition

71 of xCT by erastin) or GPX4 inhibition. Thus, the Cys–GSH–GPX4 axis appears to be
72 the primary protective system for coping with ferroptosis [2,6].

73 Nitric oxide (NO) interacts with reactive oxygen species (ROS) and is converted into
74 several reactive nitrogen oxide species, which can irreversibly modify DNA, proteins,
75 lipids and other biomolecules. For example, NO interacts with superoxide at a similar or
76 even faster rate than the dismutation reaction catalyzed by superoxide dismutase (SOD)
77 and results in the formation of peroxynitrite ($ONOO^-$) [7]. Peroxynitrite has been
78 shown to induce cellular injury through the oxidative modification of DNA, lipids, and
79 proteins [8,9]. The initiation of lipid peroxidation by the action of peroxynitrite appears
80 to play major roles in variety of diseases, as has been suggested for atherosclerosis [10].
81 For this (and other) reason, NO is often considered to be a toxic species. However, NO
82 has also been shown to abate oxidative injury in several experimental models [11][12].
83 Indeed, it has been reported that NO potently inhibits lipid peroxidation in low-density
84 lipoprotein and liposome membranes [13–15]. This is primarily a consequence of NO
85 reacting with lipid-derived peroxy radicals ($LOO\cdot$) to terminate lipid peroxidation
86 propagation reactions [16,17]. NO has also been shown to form an iron-nitrosyl

complex and inhibit the reaction between a peroxide and a metal ion, thereby preventing ROS production [18].

The issue of whether NO exerts either harmful or beneficial to cells has been a subject of considerable debate, and may also depend on the experimental conditions being used. In the current study, we examined the anti-ferroptotic properties of NOC18, a long-lasting NO donor that spontaneously releases NO under various ferroptotic conditions in cultured cells. Herein we report on the potential roles of NO in coping with ferroptotic cell death, which appears to be achieved by the suppression of ROS production and the termination of the lipid peroxidation reaction by NO.

2. Materials and methods

2.1. Cell culture and chemicals

Hepa 1-6 cells, a mouse hepatoma-derived cell line, were obtained from the RIKEN Bioresource Center (Tsukuba, Japan). The human cervical carcinoma HeLa cells and mouse melanoma B16-F1 cells were obtained from the American Type Culture Collection (ATCC). Mouse embryonic fibroblasts capable of undergoing tamoxifen-inducible GPX4 disruption (Pfa1 cells) were described in a previous report [19]. In all cases, the cells were maintained in Dulbecco's Modified Eagle's Medium (DMEM; FUJIFILM Wako Pure Chemical, Osaka, Japan; 044-29765) supplemented with 10% fetal bovine serum (FBS; Biowest, Riverside, MO, USA) and a penicillin-streptomycin solution (FUJIFILM Wako Pure Chemical; 168-23191) at 37°C in a 5% CO_2 incubator. For Cys starvation, cystine-free medium was prepared by using DMEM/high glucose/no glutamine/ no methionine/ no cystine (Thermo Fisher Scientific, Waltham, MA, USA) supplemented back with 4 mM L-glutamine (FUJIFILM Wako Pure Chemical), 1 mM sodium pyruvate (FUJIFILM Wako Pure

Chemical), and 0.2 mM L-methionine (PEPTIDE INSTITUTE, Osaka, Japan). Where indicated, the cells were treated with dimethyl sulfoxide (DMSO; FUJIFILM Wako Pure Chemical) as a vehicle control, erastin (Cayman Chemical, Ann Arbor, MI, USA), (1S, 3R)-RSL3 (Cayman Chemical), tert-butyl hydroperoxide (TBHP; FUJIFILM Wako Pure Chemical), NOC7 (Dojindo, Kumamoto, Japan), or diethylenetriamine NONOate (NOC18: Cayman Chemical).

2.2 Treatment with NO donors

Two NO donors (NOC7 and NOC18) with different half times of NO release (~5 min and >1200 min, respectively) were dissolved in 0.1 mM NaOH to produce a stock solution of 100 mM. The NOC18 solution was diluted with culture medium and applied for the cells simultaneously with the ferroptotic stimuli. To rule out the possible involvement of NOC7 degradation products other than NO, TBHP (20 μM) was first incubated with varying concentrations of NOC7 in the medium for 30 min at 37°C, and the cells were treated with the resulting TBHP.

130 *2.3. Evaluation of the viability and cytotoxicity of cells*

131 Cells were seeded at an initial density of (1×10^5/ml). Cell viability was determined
132 using a CellTiter-Blue® Cell Viability Assay (Promega, Madison, WI, USA) according
133 to the manufacturer's instructions. Fluorescence intensities were measured using a
134 microplate reader Varioskan Flash (Thermo Fisher Scientific) with an excitation
135 wavelength of 560 nm and an emission wavelength of 590 nm.

136 Cytotoxicity was determined by means of a lactate dehydrogenase (LDH) assay as
137 described previously [20]. The reaction mixture contained 20 µl of culture medium, 0.3
138 mM NADH, 1 mM sodium pyruvate, and 200 mM sodium phosphate buffer, at pH 7.4
139 in a total volume of 100 µl. Initial activities were calculated from the rate of
140 disappearance of NADH during the starting linear phase of the reaction by monitoring
141 the absorbance at 340 nm.

142

143 *2.4. Hoechst and propidium iodide (PI) double staining*

144 Cells were incubated with Hoechst 33342 and PI in the medium (2 μg/ml each) for 20
145 min at 37°C in a 5% CO_2 incubator. The cells were then washed and images were
146 obtained using a BZ-X700 microscope (KEYENCE, Osaka, Japan).
147
148 *2.5. Liquid chromatography-mass spectrometry (LC-MS) analyses*
149 LC-MS analyses of the intracellular Cys and GSH levels were performed as described
150 previously [20]. System control, data acquisition, and quantitative analysis were
151 performed with the Xcalibur 2.2 software (Thermo Fisher Scientific). Standard curves
152 for amino acids, GSH-NEM, and cysteine-NEM showed linearity in the concentration
153 ranges examined.
154
155 *2.6. Western blotting*
156 Cells were lysed in cold lysis buffer (50 mM Tris-HCl pH 7.5, 150 mM NaCl, 1%
157 NP-40, 0.1% SDS, 0.5% sodium deoxycholate), supplemented with a protease inhibitor
158 cocktail (Sigma-Aldrich; P8340). The lysate was centrifuged at 15,000 × g for 10 min in
159 a microcentrifuge and protein concentrations were then determined using a Pierce BCA

Protein Assay Kit (Thermo Fisher Scientific). The proteins were separated on SDS–polyacrylamide gels and blotted onto polyvinylidene difluoride (PVDF) membranes (GE Healthcare, Chicago, IL, USA). The blots were then blocked with 5% skim milk in Tris-buffered saline containing 0.1% Tween-20 (TBST), and incubated overnight with the primary antibodies diluted in TBST. The antibodies used in the study were GPX4 (Abcam, Cambridge, UK; ab125066, 1:1000 dilution) and β-actin (GeneTex; GTX629630, 1:2000 dilution). After three washings with TBST, the blots were incubated with horseradish peroxidase (HRP)-conjugated anti-rabbit (Santa Cruz Biotechnology; sc-2004) or anti-mouse (Santa Cruz Biotechnology; sc-2005) secondary antibodies. After further washing, the bands were detected using the Immobilon western chemiluminescent HRP substrate (Merck Millipore, Burlington, MA, USA) on an image analyzer (ImageQuant LAS500, GE Healthcare).

2.7. Flow cytometry

Cells were incubated with 10 μM C11-BODIPY$^{581/591}$ (Thermo Fisher Scientific) for 30 min or 5 μM FerroFarRed (Goryochemical, Hokkaido, Japan) for 1 h following the

manufacturer's instructions and then washed with PBS. After trypsinization, the cells were collected and subjected to flow cytometry (FACSCanto™ II, BD Biosciences, Tokyo, Japan).

2.8. Real-time PCR analyses

RNA from the Hepa 1-6 cells was purified by means of the TRIzol® Reagent (Thermo Fisher Scientific). cDNA was prepared with a PrimeScript™ RT reagent Kit (TaKaRa Bio, Shiga, Japan). Real-time PCR analysis was performed by using Thunderbird SYBR qPCR mix (TOYOBO, Osaka, Japan) and previously reported primers [21] on a CFX-96 Real-time system (Bio-Rad, Hercules, CA, USA). GAPDH was used as a reference gene and was amplified using the sense primer 5'-AACTTTGGCATTGTGGAAGG-3' and antisense primer 5'-GGATGCAGGGATGATGTTCT-3'.

2.9. Immunostaining

Cells were washed with PBS and fixed in 4% formaldehyde for 15 min at room

192 temperature. After washing twice with PBS, the cells were permeabilized for 5 min by
193 treatment with 0.5 % Triton X-100 in PBS, then blocked for 30 min by treatment with
194 1% BSA in PBS at room temperature, followed by incubation overnight with 10 μg/mL
195 FerAb [22] or anti-HNE (JaICA, Fukuroi, Japan, dilution 1:500) antibodies at 4°C.
196 After three washes with PBS, the cells were further incubated with a goat anti-rat IgG
197 (H+L) or goat anti-mouse IgG (H+L) Alexa Fluor® 488 conjugate antibody (Thermo
198 Fisher Scientific, dilution 1:500) for 60 min at room temperature. All images were
199 obtained using a BZ-X700 microscope (KEYENCE).
200

201 *2.10. Statistical analysis*

202 Statistical analyses were performed using the GraphPad Prism version 6.0 for Mac (San
203 Diego, CA, USA). A *P*-value of less than 0.05 was considered to be significant.
204

205 **3. Results**

206 *3.1. NOC18 treatment inhibits ferroptosis induced by Cys starvation*

207 To investigate the potential role of NO in protecting cells against ferroptosis, we
208 treated mouse hepatoma-derived Hepa 1-6 cells with a long-lasting NO donor. NOC18
209 (half-life >1200 min). A CellTiter-Blue® assay showed that depriving cystine from the
210 culture media resulted in a decreased cell viability, while the administration of NOC18
211 improved cell viability at concentrations higher than 25 μM (Fig. 1A). An assay for the
212 release of LDH confirmed that NOC18 suppressed the ferroptotic cell death caused by
213 the cystine deprivation (Fig. 1B). Staining the cells with PI (propidium iodide) that
214 binds to DNA in dead cells with leaky plasma membranes revealed that the NOC18
215 caused a decrease in the numbers of PI-positive cells, the concentrations of which were
216 elevated in the cystine-deprivation cultures (Fig. 1C).

217 We also treated the Hepa 1-6 cells with erastin, a potent inhibitor of xCT, and found
218 that NOC18 again rescued cells from the ferroptosis caused by the erastin treatment at
219 concentrations higher than 10 μM (Fig. 1D). The protective action of NOC18 under the
220 erastin treatment was further confirmed by an LDH release assay (Fig. 1E) and PI

staining (Fig. 1F). Similar results were obtained in human cervix carcinoma HeLa cells and mouse melanoma B16-F1 cells (Supplementary Fig. 1A–D), indicating that the action of NOC18 was not cell-type specific.

To exclude the possibility that NOC18 suppresses ferroptosis via stimulating the recruitment of Cys and/or GSH synthesis, we measured the intracellular levels of Cys and GSH. The results indicated that their levels were decreased to a considerable extent at 24 h after cystine deprivation, but that NOC18 failed to improve the decreased levels of Cys or GSH (Fig. 2A). Again, NOC18 had no effect on either the GSH or Cys levels when Hepa 1-6 cells were treated with erastin (Fig. 2B).

It has been reported by several researchers that GPX4 is down-regulated during ferroptosis [23,24]. It has also been reported that GPX4 is degraded by chaperone-mediated autophagy during ferroptosis [25]. To examine a possible association between the protective action of NOC18 and the function of GPX4, we examined the levels of the GPX4 protein by western blotting. Both cystine deprivation and the erastin treatment promoted the down-regulation of GPX4, which was slightly rescued by a NOC18 treatment (Figs. 2C and 2D). Because NOC18 alone had no effects

237 on the GPX4 protein levels, the sustained levels of the GPX4 protein appears to be a
238 consequence of the suppressive action of NO on the ferroptotic process, which
239 reportedly is accompanied by the autophagic degradation of GPX4 [26].
240
241 *3.2. NOC18 does not alter iron status during ferroptosis*
242 Since lipid peroxidation and the subsequent ferroptotic processes are associated with
243 the accumulation of free ferrous iron and the fact that NO can, in some instances, inhibit
244 iron-mediated ROS production by forming an iron-nitrosyl complex [18], we explored
245 effects of NOC18 on iron mobilization in the cells by means of flow cytometry using a
246 ferrous iron-specific fluorescent probe FerroFarRed. We found that both cystine
247 deprivation and the erastin treatment resulted in a substantial increase in the levels of
248 intracellular ferrous iron (Fig. 3A), consistent with the decreased cellular viability.
249 However, the co-treatment with NOC18 had no suppressive effect on these elevations.
250 To investigate the effect of NOC18 on the expression of four key genes that are
251 involved in iron metabolism, Hepa 1-6 cells were treated with 100 μM NOC18 for 8 h
252 under Cys-deprived culture or in the presence of erastin, and the mRNA levels of

transferrin receptor 1 (*Tfrc*), the divalent metal transporter 1 (*Dmt1*), ferroportin (*Fpn*), and ferritin heavy chain (*Fth1*) were then determined. There were no significant changes in the expressions of these genes (Fig. 3B), suggesting that the NOC18 treatment did not directly modulate the level of expression of these genes.

3.3. NOC18 aborts ferroptosis by terminating the lipid peroxidation chain reaction

To further clarify the mechanism responsible for the protective action of NOC18 against ferroptosis, we examined the issue of whether NOC18 could suppress lipid peroxidation in the cells using C11-BODIPY$^{581/591}$, a fluorescent probe that is typically used to detect lipid peroxidation products, by a flow cytometry. While the fluorescent intensity was elevated in the cells that were cultivated in the cystine-free medium or in the presence of erastin, NOC18 failed to suppress the fluorescent intensity in these Cys-starved cells, and instead, elevated it somewhat (Fig. 4A). NOC18 alone did not increase C11-BODIPY$^{581/59}$ fluorescence under control conditions, indicating that the elevated fluorescence was not due to the direct action of NO. Therefore, we next measured the intracellular levels of adducts with 4-hydroxynonenal (4-HNE), one of the

end products of lipid peroxidation, using a specific antibody (HNE Ab) by immunofluorescent staining. While both cystine deprivation and the erastin treatment caused significant increases in the accumulation of 4-HNE-adducts, NOC18 caused a significant suppression in these elevations (Fig. 4B). For further confirmation, we used the ferroptosis-specific antibody (FerAb) that was developed recently in our laboratory [22]. Both cystine deprivation and the erastin treatment also caused an increase in the binding of FerAb to the cells under these conditions, and NOC18 again effectively suppressed this binding (Fig. 4C). It therefore appears that NOC18 did not suppress the formation of C11-BODIPY$^{581/591}$-reactive substances, which were elevated under ferroptotic stimuli, but, rather, enhanced their production. However, the reactivity to the antibodies declined, suggesting that NOC18 suppressed the progression of lipid peroxidation and the subsequent formation of the end products.

3.4. NOC18 treatment inhibits ferroptosis induced by GPX4 inhibition

To investigate the possible association between the protective action of NOC18 and GPX4 function, we next examined the issue of whether NOC18 could rescue the

285 ferroptosis induced by RSL3, a pharmacological inhibitor of GPX4. The lethal effects of
286 RSL3 were suppressed by NOC18, as evidenced by the LDH assay (Fig. 5A) and by PI
287 staining (Fig. 5B). The protective effect against the GPX4 inhibition was also confirmed
288 in HeLa and B16-F1 cells (Supplementary Fig. 1). We also found that FerAb binding
289 was decreased when RSL3-induced ferroptosis was suppressed by a treatment with
290 NOC18 (Fig. 5B), although NOC18 failed to suppress the fluorescent intensity of
291 C11-BODIPY$^{581/591}$ in RSL3-treated Hepa 1-6 cells again (Fig. 5C).

292 To further assess the protective effect of NOC18 against the ferroptosis triggered by
293 GPX4 inhibition, we utilized tamoxifen-inducible GPX4 knockout Pfa1 cells [19]. In
294 these cells, treatment with tamoxifen caused the simultaneous depletion of GPX4 and
295 ferroptosis (Figs. 5E and 5F), whereas treatment with NOC18 suppressed ferroptosis
296 but had no effect on the level of the GPX4 protein, which was consistent with the results
297 for GPX4 inhibition when using RSL3 in Hepa 1-6 cells (Fig. 5A). These collective
298 results suggest that the NO released from NOC18 exerted an anti-ferroptotic action by
299 aborting the ongoing lipid peroxidation reaction even under GPX4 inhibition.
300

301 *3.5. NOC18 treatment inhibits the ferroptosis induced by TBHP treatment*

302 *Tert*-butyl hydroperoxide (TBHP) non-enzymatically leads to the formation of
303 primary alkoxyl- (TBO·) and secondarily peroxyl radicals (TBOO·), which abstract
304 hydrogen from polyunsaturated fatty acids thereby initiating lipid peroxidation [27–29],
305 and reportedly induces ferroptosis [30,31]. We next examined the issue of whether
306 NOC18 could rescue the ferroptosis induced by TBHP. As a result, the protective action
307 of NOC18 against ferroptosis under the TBHP treatment was confirmed by an LDH
308 assay (Fig. 6A), PI staining (Fig. 6B) and immunofluorescence assay using FerAb (Fig.
309 6B). To confirm that NO itself reacted with TBHP-derived radical species and thereby
310 prevented the radical chain reaction, TBHP was incubated with another NO donor,
311 NOC7, which has a very short half-life (~5 min), for 30 min at room temperature. We
312 then treated the cells with TBHP or TBHP that had been preincubated with NOC7 and
313 found that the pre-incubation with NOC7 significantly suppressed the release of LDH in
314 a NOC7 dose-dependent manner (Fig. 6C). Because when TBHP was pre-incubated
315 with a decomposition product of NOC7, ferroptosis continued to be induced, these
316 collective results imply that NO released from the donor compound reacted with

317 TBHP-derived radical species and thereby prevented the lipid peroxidation chain

318 reaction from proceeding.

319

4. Discussion

In the current study, we showed that NO produced by an NO donor NOC18 exerts protective effects against ferroposis caused by diverse stimuli, including Cys starvation, GPX4 inhibition and a TBHP treatment (Figs. 1, 5, and 6). NO failed to prevent the decrease in cellular Cys or GSH levels but still suppressed ferroptosis under Cys starvation (Fig. 2). Although the levels of the GPX4 protein, which were decreased under Cys starvation, were partly rescued by the NOC18 treatment, it failed to reduce the levels of phospholipid hydroperoxides due to a GSH insufficiency. These collective data indicate that NO-mediated protection is based on a mechanism that is different from that for the Cys-GSH-GPX4 axis. When TBHP was pre-incubated with a short-lived NO donor, NOC7, the induction of ferroptosis by TBHP was completely abolished (Fig. 6). These results imply that interactions between NO and TBHP-derived peroxy radicals greatly inhibited the progress of the radical chain reaction. These collective results suggest that the abortion of the lipid peroxidation reaction by NO is the most likely mechanism for this protection against ferroptosis, although other mechanisms including the conversion of superoxide, which could serve as the primary

source of electrons for lipid peroxidation in cystine starvation-induced ferroptosis [32], to peroxynitrite may also be responsible for the NO-medicated suppression of ferroptosis.

NO preferentially binds iron, heme, and thiols and therefore may affect a variety of metabolic reactions. As a result, there are many potential reactions that could be targets of NO, which consequently leads to the suppression of ferroptosis. The formation of hydroxyl radicals or metal-oxo species often depends on the presence of ferrous iron. The transfer of an unpaired electron of superoxide to another molecule may result in the production of hydroxyl radicals by means of the reduction of ferric iron to ferrous iron (Haber–Weiss chemistry) [33]. Because NO affects cellular iron status in multiple manners, such as the formation of a complex with iron or the release of free iron [34], the possibility that NO suppresses ferroptosis via decreasing the content of reactive free iron cannot be excluded. It is noteworthy, however that we were unable to provide evidence that the NOC18 treatment decreased ferrous iron content or modulated the expression of genes involved in iron metabolism (Fig. 3). Thus,

351 detoxification via the removal of free iron would be unlikely mechanism for
352 suppressing ferroptosis by NO.

353 Because hydrogen peroxide, which allows the Fenton reaction to proceed in the
354 presence of free iron, is generally derived from superoxide, the production of excessive
355 superoxide levels enhances the lipid peroxidation chain reaction [35]. Shunting
356 superoxide to peroxynitrite followed by nitrate formation thus inhibits the reduction of
357 ferric iron to ferrous iron and prevents the catalytic formation of ROS and lipid
358 peroxidation products. This may also be an important mechanism for the abatement of
359 Fenton-type reaction-mediated oxidative stress by NO. Although NO is a well known
360 and effective superoxide scavenger, it has been suggested that the resulting peroxynitrite
361 is still highly reactive and is capable of exerting oxidative damage [36]. In fact, the
362 issue of whether the reaction between NO and superoxide becomes beneficial or
363 harmful to cells depends on the relative rate of production of the two radicals [37,38];
364 an excess of NO favors the inhibition of lipid peroxidation while an excess of
365 superoxide or other reactive oxygen radicals induces lipid peroxidation [39]. We
366 recently reported that the viability of macrophages from knockout mice for superoxide

dismutase 1 (SOD1) is markedly ameliorated by both an exogenous NO donor and endogenously produced NO, despite an increase in the production of peroxynitrite [40]. These results indicate that, when increasing the rates of NO formation flux exceeds the superoxide flux, NO overcomes the cytotoxic effects of superoxide and eventually ferroptosis, most likely due to its superoxide-scavenging function.

The increase in lipid peroxidation products detected by C11-BODIPY$^{581/591}$ (Fig. 4A and 5C) was a unique observation for the NO-mediated suppression of ferroptosis and was not seen in other anti-ferroptotic events. Chemical compounds, such as ferrostatin-1 and edaravone, and gene products, such as GPX4 and FSP1 (Doll et al., 2019), generally decrease lipid peroxidation levels directly or indirectly and result in the suppression of ferroptosis. The antioxidant effect of NO on lipid peroxidation has been explained by terminating the radical chain reaction through the reaction of NO with lipid peroxy radicals to form less reactive secondary nitrogen-containing products such as LONO and LOONO [16,17]. C11-BODIPY$^{581/591}$ is sensitive to a variety of oxy-radicals and peroxynitrite in a lipophilic environment, but not to superoxide, NO, transition metal ions, or peroxides per se [41]. The constant production of superoxide

383 from the mitochondrial electron transport chain [32], notably from complex III [42],
384 reportedly promotes ferroptosis under conditions of Cys starvation. Thus, the
385 simultaneous presence of superoxide and NO would be expected to form peroxynitrite,
386 which may partly contribute to the elevated fluorescence of C11-BODIPY$^{581/591}$
387 reported in this study. Otherwise, the C11-BODIPY$^{581/591}$ would still react with some
388 currently unknown reactive species, while the chain termination of lipid peroxidation
389 was ceased by NO.

390 NO is endogenously synthesized by a family of NO synthases (NOS). Among the
391 three isoforms of NOS, inducible NOS (NOS2) is closely related to inflammatory and
392 autoimmune diseases [43]. Lipoxygenase, which mediates a variety of lipid oxidation
393 reactions in inflammatory cells, is inhibited by NO [44]. Arachidonate-15-lipoxygenase
394 (Alox15) is involved in lipid peroxidation during ferroptosis in response to erastin and
395 GPX4 inhibition [45]. It has been recently reported that NO could interact with a
396 reactive intermediate of 15-lipoxygenase or lipid radical intermediates in ferroptotic
397 macrophages triggered by RSL3, leading to the suppression of the execution of
398 ferroptosis in these cells [46]. In the current study, we attempted to evaluate the

399 protective effects of NOC18 against ferroptosis triggered by various ferroptotic stimuli
400 in non-inflammatory cells. In addition to ferroptsosis caused by Cys deprivation,
401 indeed, ferroptosis induced by TBHP was also rescued by the NOC18 treatment, where
402 the cell death mode has been reported to be Alox15-independent [30,31] but ferrous
403 iron-dependent [47].

404 From the physiological standpoint, since NOS2 is a high-output NOS compared
405 with the other NOS isoforms, the production of excessive levels of NO by NOS2 would
406 be able to exert an anti-ferroptosis action, as previously reported [46]. However, a lower
407 amount of NO produced by NOS1 or NOS3 under physiological conditions may not
408 allow for an assessment of the protective effects of endogenous NO against ferrpotosis
409 that is induced under conditions of severe ferropttic stimuli. While the induction of
410 ferroptosis in malignant cells has attracted considerable interest as related to cancer
411 treatment, in some tumors, NO reportedly protects cancer cells against photo-killing
412 during photodynamic therapy (PDT) [48]. We previously reported that ferroptosis is the
413 cell death pathway induced by singlet oxygen [49], which is the main form of reactive
414 oxygen responsible for tumor-cell killing by PDT. Given the fact that NO is produced as

one of the anti-ferroptotic events under PDT, the inhibition of NOS may improve the treatment outcome for PDT. In contrast, ferroptosis is reportedly involved in the aggravation of pulmonary diseases such as acute lung injury [50]. In such cases, NO inhalation therapy may suppress ferroptosis and become an effective treatment.

In conclusion, the findings reported in this study provide information concerning the protective effects of NO against ferroptotic cell death under conditions of Cys starvation, GPX4 inhibition, and the direct stimulation of lipid peroxidation. Collectively, our results imply that NO has a novel role in coping with ferroptosis. Cellular susceptibility to ferroptosis appears to be associated to cancer outcomes and other ferroptosis-related diseases, and, hence, a more complete understanding of the anti-ferroptotic mechanism by NO could be useful for developing treatments that target such diseases.

Conflict of interest

The authors declare no conflicts of interest.

Acknowledgments

This work was supported, in part, by the YU-COE (C) (C31-3) program of Yamagata University. We thank Prof. Makoto Arita and Dr. Ryohei Aoyagi of Graduate School of Pharmaceutical Sciences, Keio University for their technical advice.

437

438 **References**

439 [1] S.J. Dixon, K.M. Lemberg, M.R. Lamprecht, R. Skouta, E.M. Zaitsev, C.E.
440 Gleason, D.N. Patel, A.J. Bauer, A.M. Cantley, W.S. Yang, B. Morrison, B.R.
441 Stockwell, Ferroptosis: An Iron-Dependent Form of Nonapoptotic Cell Death,
442 Cell. 149 (2012) 1060–1072. https://doi.org/10.1016/j.cell.2012.03.042.
443 [2] B.R. Stockwell, J.P. Friedmann Angeli, H. Bayir, A.I. Bush, M. Conrad, S.J.
444 Dixon, S. Fulda, S. Gascón, S.K. Hatzios, V.E. Kagan, K. Noel, X. Jiang, A.
445 Linkermann, M.E. Murphy, M. Overholtzer, A. Oyagi, G.C. Pagnussat, J. Park, Q.
446 Ran, C.S. Rosenfeld, K. Salnikow, D. Tang, F.M. Torti, S. V Torti, S. Toyokuni,
447 K.A. Woerpel, D.D. Zhang, Ferroptosis: A Regulated Cell Death Nexus Linking
448 Metabolism, Redox Biology, and Disease., Cell. 171 (2017) 273–285.
449 https://doi.org/10.1016/j.cell.2017.09.021.
450 [3] S. Toyokuni, F. Ito, K. Yamashita, Y. Okazaki, S. Akatsuka, Iron and thiol redox
451 signaling in cancer: An exquisite balance to escape ferroptosis., Free Radic. Biol.
452 Med. 108 (2017) 610–626. https://doi.org/10.1016/j.freeradbiomed.2017.04.024.
453 [4] W.S. Yang, R. SriRamaratnam, M.E. Welsch, K. Shimada, R. Skouta, V.S.
454 Viswanathan, J.H. Cheah, P.A. Clemons, A.F. Shamji, C.B. Clish, L.M. Brown,
455 A.W. Girotti, V.W. Cornish, S.L. Schreiber, B.R. Stockwell, Regulation of
456 ferroptotic cancer cell death by GPX4., Cell. 156 (2014) 317–331.
457 https://doi.org/10.1016/j.cell.2013.12.010.
458 [5] M. Conrad, H. Sato, The oxidative stress-inducible cystine/glutamate antiporter,
459 system x (c) (-) : cystine supplier and beyond., Amino Acids. 42 (2012) 231–46.
460 https://doi.org/10.1007/s00726-011-0867-5.
461 [6] J. Fujii, T. Homma, S. Kobayashi, Ferroptosis caused by cysteine insufficiency
462 and oxidative insult., Free Radic. Res. (2019) 1–12.
463 https://doi.org/10.1080/10715762.2019.1666983.
464 [7] R. Radi, Peroxynitrite, a Stealthy Biological Oxidant, J. Biol. Chem. 288 (2013)
465 26464–26472. https://doi.org/10.1074/jbc.R113.472936.
466 [8] C. Szabó, H. Ohshima, DNA damage induced by peroxynitrite: subsequent
467 biological effects., Nitric Oxide Biol. Chem. 1 (1997) 373–85.

https://doi.org/10.1006/niox.1997.0143.

[9] T. Nguyen, D. Brunson, C.L. Crespi, B.W. Penman, J.S. Wishnok, S.R. Tannenbaum, DNA damage and mutation in human cells exposed to nitric oxide in vitro, Proc. Natl. Acad. Sci. U. S. A. 89 (1992) 3030–3034. https://doi.org/10.1073/pnas.89.7.3030.

[10] C.R. White, T.A. Brock, L.Y. Chang, J. Crapo, P. Briscoe, D. Ku, W.A. Bradley, S.H. Gianturco, J. Gore, B.A. Freeman, Superoxide and peroxynitrite in atherosclerosis., Proc. Natl. Acad. Sci. U. S. A. 91 (1994) 1044–8. https://doi.org/10.1073/pnas.91.3.1044.

[11] D.A. Wink, I. Hanbauer, M.C. Krishna, W. DeGraff, J. Gamson, J.B. Mitchell, Nitric oxide protects against cellular damage and cytotoxicity from reactive oxygen species, Proc. Natl. Acad. Sci. U. S. A. 90 (1993) 9813–9817. https://doi.org/10.1073/pnas.90.21.9813.

[12] M. Godínez-Rubí, A.E. Rojas-Mayorquín, D. Ortuño-Sahagún, Nitric oxide donors as neuroprotective agents after an ischemic stroke-related inflammatory reaction., Oxid. Med. Cell. Longev. 2013 (2013) 297357. https://doi.org/10.1155/2013/297357.

[13] W. Jessup, D. Mohr, S.P. Gieseg, R.T. Dean, R. Stocker, The participation of nitric oxide in cell free- and its restriction of macrophage-mediated oxidation of low-density lipoprotein, Biochim. Biophys. Acta - Mol. Basis Dis. 1180 (1992) 73–82. https://doi.org/10.1016/0925-4439(92)90029-M.

[14] U. Malo-Ranta, S. Ylä-Herttuala, T. Metsä-Ketelä, O. Jaakkola, E. Moilanen, P. Vuorinen, T. Nikkari, Nitric oxide donor GEA 3162 inhibits endothelial cell-mediated oxidation of low density lipoprotein., FEBS Lett. 337 (1994) 179–83. https://doi.org/10.1016/0014-5793(94)80269-6.

[15] K. Hayashi, N. Noguchi, E. Niki, Action of nitric oxide as an antioxidant against oxidation of soybean phosphatidylcholine liposomal membranes, FEBS Lett. 370 (1995) 37–40. https://doi.org/10.1016/0014-5793(95)00786-9.

[16] V.B. O'Donnell, P.H. Chumley, N. Hogg, A. Bloodsworth, V.M. Darley-Usmar, B.A. Freeman, Nitric oxide inhibition of lipid peroxidation: kinetics of reaction with lipid peroxyl radicals and comparison with alpha-tocopherol., Biochemistry. 36 (1997) 15216–23. https://doi.org/10.1021/bi971891z.

[17] V.B. O'Donnell, J.P. Eiserich, A. Bloodsworth, P.H. Chumley, M. Kirk, S. Barnes, V.M. Darley-Usmar, B.A. Freeman, Nitration of unsaturated fatty acids by nitric oxide-derived reactive species., Methods Enzymol. 301 (1999) 454–70. https://doi.org/10.1016/s0076-6879(99)01109-x.

[18] D.A. Wink, K.M. Miranda, M.G. Espey, R.M. Pluta, S.J. Hewett, C. Colton, M. Vitek, M. Feelisch, M.B. Grisham, Mechanisms of the antioxidant effects of nitric oxide., Antioxid. Redox Signal. 3 (2001) 203–13. https://doi.org/10.1089/152308601300185179.

[19] A. Seiler, M. Schneider, H. Förster, S. Roth, E.K. Wirth, C. Culmsee, N. Plesnila, E. Kremmer, O. Rådmark, W. Wurst, G.W. Bornkamm, U. Schweizer, M. Conrad, Glutathione peroxidase 4 senses and translates oxidative stress into 12/15-lipoxygenase dependent- and AIF-mediated cell death., Cell Metab. 8 (2008) 237–48. https://doi.org/10.1016/j.cmet.2008.07.005.

[20] T. Homma, S. Kobayashi, H. Sato, J. Fujii, Edaravone, a free radical scavenger, protects against ferroptotic cell death in vitro., Exp. Cell Res. 384 (2019) 111592. https://doi.org/10.1016/j.yexcr.2019.111592.

[21] H.J. Chen, M. Sugiyama, F. Shimokawa, M. Murakami, O. Hashimoto, T. Matsui, M. Funaba, Response to iron overload in cultured hepatocytes, Sci. Rep. 10 (2020) 1–11. https://doi.org/10.1038/s41598-020-78026-6.

[22] S. Kobayashi, Y. Harada, T. Homma, C. Yokoyama, J. Fujii, Characterization of a rat monoclonal antibody raised against ferroptotic cells., J. Immunol. Methods. 489 (2021) 112912. https://doi.org/10.1016/j.jim.2020.112912.

[23] S. Zhu, Q. Zhang, X. Sun, H.J. Zeh, M.T. Lotze, R. Kang, D. Tang, HSPA5 Regulates Ferroptotic Cell Death in Cancer Cells., Cancer Res. 77 (2017) 2064–2077. https://doi.org/10.1158/0008-5472.CAN-16-1979.

[24] K. Shimada, R. Skouta, A. Kaplan, W.S. Yang, M. Hayano, S.J. Dixon, L.M. Brown, C.A. Valenzuela, A.J. Wolpaw, B.R. Stockwell, Global survey of cell death mechanisms reveals metabolic regulation of ferroptosis., Nat. Chem. Biol. 12 (2016) 497–503. https://doi.org/10.1038/nchembio.2079.

[25] Z. Wu, Y. Geng, X. Lu, Y. Shi, G. Wu, M. Zhang, B. Shan, H. Pan, J. Yuan, Chaperone-mediated autophagy is involved in the execution of ferroptosis., Proc. Natl. Acad. Sci. U. S. A. 116 (2019) 2996–3005.

https://doi.org/10.1073/pnas.1819728116.

[26] Z. Wu, Y. Geng, X. Lu, Y. Shi, G. Wu, M. Zhang, B. Shan, H. Pan, J. Yuan, Chaperone-mediated autophagy is involved in the execution of ferroptosis, Proc. Natl. Acad. Sci. 116 (2019) 2996–3005. https://doi.org/10.1073/pnas.1819728116.

[27] D.P. Barr, R.P. Mason, Mechanism of Radical Production from the Reaction of Cytochrome c with Organic Hydroperoxides., J. Biol. Chem. 270 (1995) 12709–12716. https://doi.org/10.1074/jbc.270.21.12709.

[28] S. Hix, M.B. Kadiiska, R.P. Mason, O. Augusto, In Vivo Metabolism of tert -Butyl Hydroperoxide to Methyl Radicals. EPR Spin-Trapping and DNA Methylation Studies, Chem. Res. Toxicol. 13 (2000) 1056–1064. https://doi.org/10.1021/tx000130l.

[29] N. Masaki, M.E. Kyle, J.L. Farber, tert-Butyl hydroperoxide kills cultured hepatocytes by peroxidizing membrane lipids, Arch. Biochem. Biophys. 269 (1989) 390–399. https://doi.org/10.1016/0003-9861(89)90122-7.

[30] L. Jiang, N. Kon, T. Li, S.-J. Wang, T. Su, H. Hibshoosh, R. Baer, W. Gu, Ferroptosis as a p53-mediated activity during tumour suppression., Nature. 520 (2015) 57–62. https://doi.org/10.1038/nature14344.

[31] C. Wenz, D. Faust, B. Linz, C. Turmann, T. Nikolova, J. Bertin, P. Gough, P. Wipf, A.S. Schröder, S. Krautwald, C. Dietrich, t-BuOOH induces ferroptosis in human and murine cell lines., Arch. Toxicol. 92 (2018) 759–775. https://doi.org/10.1007/s00204-017-2066-y.

[32] M. Gao, J. Yi, J. Zhu, A.M. Minikes, P. Monian, C.B. Thompson, X. Jiang, Role of Mitochondria in Ferroptosis, Mol. Cell. 73 (2019) 354-363.e3. https://doi.org/10.1016/j.molcel.2018.10.042.

[33] M.R. Filipovic, W.H. Koppenol, The Haber-Weiss reaction - The latest revival., Free Radic. Biol. Med. 145 (2019) 221–222. https://doi.org/10.1016/j.freeradbiomed.2019.09.017.

[34] Y. Henry, M. Lepoivre, J. Drapier, C. Ducrocq, J. Boucher, A. Guissani, EPR characterization of molecular targets for NO in mammalian cells and organelles, FASEB J. 7 (1993) 1124–1134. https://doi.org/10.1096/fasebj.7.12.8397130.

[35] E. Niki, Lipid peroxidation: Physiological levels and dual biological effects, Free

564 Radic. Biol. Med. 47 (2009) 469–484.
565 https://doi.org/10.1016/j.freeradbiomed.2009.05.032.
566 [36] R.E. Huie, S. Padmaja, The Reaction of no With Superoxide, Free Radic. Res.
567 Commun. 18 (1993) 195–199. https://doi.org/10.3109/10715769309145868.
568 [37] D.A. Wink, J.A. Cook, S.Y. Kim, Y. Vodovotz, R. Pacelli, M.C. Krishna, A.
569 Russo, J.B. Mitchell, D. Jourd'heuil, A.M. Miles, M.B. Grisham, Superoxide
570 modulates the oxidation and nitrosation of thiols by nitric oxide-derived reactive
571 intermediates. Chemical aspects involved in the balance between oxidative and
572 nitrosative stress, J. Biol. Chem. 272 (1997) 11147–11151.
573 https://doi.org/10.1074/jbc.272.17.11147.
574 [38] H. Rubbo, R. Radi, M. Trujillo, R. Telleri, B. Kalyanaraman, S. Barnes, M. Kirk,
575 B.A. Freeman, Nitric oxide regulation of superoxide and peroxynitrite-dependent
576 lipid peroxidation. Formation of novel nitrogen-containing oxidized lipid
577 derivatives, J. Biol. Chem. 269 (1994) 26066–26075.
578 https://doi.org/10.1016/s0021-9258(18)47160-8.
579 [39] F. Violi, R. Marino, M.T. Milite, L. Loffredo, Nitric oxide and its role in lipid
580 peroxidation., Diabetes. Metab. Res. Rev. 15 (n.d.) 283–8.
581 https://doi.org/10.1002/(sici)1520-7560(199907/08)15:4<283::aid-dmrr42>3.0.co
582 ;2-u.
583 [40] S. Kobayashi, T. Homma, J. Fujii, Nitric oxide produced by NOS2 copes with the
584 cytotoxic effects of superoxide in macrophages., Biochem. Biophys. Reports. 26
585 (2021) 100942. https://doi.org/10.1016/j.bbrep.2021.100942.
586 [41] G.P.. Drummen, L.C.. van Liebergen, J.A.. Op den Kamp, J.A. Post,
587 C11-BODIPY581/591, an oxidation-sensitive fluorescent lipid peroxidation
588 probe: (micro)spectroscopic characterization and validation of methodology, Free
589 Radic. Biol. Med. 33 (2002) 473–490.
590 https://doi.org/10.1016/S0891-5849(02)00848-1.
591 [42] T. Homma, S. Kobayashi, H. Sato, J. Fujii, Superoxide produced by mitochondrial
592 complex III plays a pivotal role in the execution of ferroptosis induced by cysteine
593 starvation., Arch. Biochem. Biophys. 700 (2021) 108775.
594 https://doi.org/10.1016/j.abb.2021.108775.
595 [43] S. Anavi, O. Tirosh, iNOS as a metabolic enzyme under stress conditions., Free

596 Radic. Biol. Med. 146 (2020) 16–35.
597 https://doi.org/10.1016/j.freeradbiomed.2019.10.411.
598 [44] D.A. Wink, J.B. Mitchell, Chemical biology of nitric oxide: Insights into
599 regulatory, cytotoxic, and cytoprotective mechanisms of nitric oxide, Free Radic.
600 Biol. Med. 25 (1998) 434–456. https://doi.org/10.1016/S0891-5849(98)00092-6.
601 [45] J.P. Friedmann Angeli, M. Schneider, B. Proneth, Y.Y. Tyurina, V.A. Tyurin, V.J.
602 Hammond, N. Herbach, M. Aichler, A. Walch, E. Eggenhofer, D. Basavarajappa,
603 O. Rådmark, S. Kobayashi, T. Seibt, H. Beck, F. Neff, I. Esposito, R. Wanke, H.
604 Förster, O. Yefremova, M. Heinrichmeyer, G.W. Bornkamm, E.K. Geissler, S.B.
605 Thomas, B.R. Stockwell, V.B. O'Donnell, V.E. Kagan, J.A. Schick, M. Conrad,
606 Inactivation of the ferroptosis regulator Gpx4 triggers acute renal failure in mice.,
607 Nat. Cell Biol. 16 (2014) 1180–91. https://doi.org/10.1038/ncb3064.
608 [46] A.A. Kapralov, Q. Yang, H.H. Dar, Y.Y. Tyurina, T.S. Anthonymuthu, R. Kim,
609 C.M. St Croix, K. Mikulska-Ruminska, B. Liu, I.H. Shrivastava, V.A. Tyurin,
610 H.-C. Ting, Y.L. Wu, Y. Gao, G. V Shurin, M.A. Artyukhova, L.A. Ponomareva,
611 P.S. Timashev, R.M. Domingues, D.A. Stoyanovsky, J.S. Greenberger, R.K.
612 Mallampalli, I. Bahar, D.I. Gabrilovich, H. Bayır, V.E. Kagan, Redox lipid
613 reprogramming commands susceptibility of macrophages and microglia to
614 ferroptotic death., Nat. Chem. Biol. 16 (2020) 278–290.
615 https://doi.org/10.1038/s41589-019-0462-8.
616 [47] K. Abe, H. Saito, Characterization of t-butyl hydroperoxide toxicity in cultured rat
617 cortical neurones and astrocytes., Pharmacol. Toxicol. 83 (1998) 40–6.
618 https://doi.org/10.1111/j.1600-0773.1998.tb01440.x.
619 [48] A.W. Girotti, Nitric Oxide-elicited Resistance to Antitumor Photodynamic
620 Therapy via Inhibition of Membrane Free Radical-mediated Lipid Peroxidation,
621 Photochem. Photobiol. (2020) 1–11. https://doi.org/10.1111/php.13373.
622 [49] T. Homma, S. Kobayashi, J. Fujii, Induction of ferroptosis by singlet oxygen
623 generated from naphthalene endoperoxide., Biochem. Biophys. Res. Commun.
624 518 (2019) 519–525. https://doi.org/10.1016/j.bbrc.2019.08.073.
625 [50] Y. Li, Y. Cao, J. Xiao, J. Shang, Q. Tan, F. Ping, W. Huang, F. Wu, H. Zhang, X.
626 Zhang, Inhibitor of apoptosis-stimulating protein of p53 inhibits ferroptosis and
627 alleviates intestinal ischemia/reperfusion-induced acute lung injury, Cell Death

628 Differ. 27 (2020) 2635–2650. https://doi.org/10.1038/s41418-020-0528-x.

629

630

631 **Figure legends**

632 **Fig. 1. Effects of NOC18 on ferroptosis induced by Cys starvation in Hepa 1-6**

633 **cells.**

634 (A) Cell viability was assessed by CellTiter-Blue assay. Hepa 1-6 cells were incubated

635 in conventional or cystine-free medium for 24 h in the presence or absence of

636 NOC18 at the indicated concentrations. Data represent the mean ± SEM (n = 4).

637 ***$p < 0.001$ (Dunnett's test, vs. cystine-free without NOC18). *n.s.*, not significant.

638 (B) Cytotoxicity of cells assessed by measuring released LDH activity. Hepa 1-6 cells

639 were incubated in conventional or cystine-free medium for 24 h in the presence or

640 absence of 100 μM NOC18. Data represent the mean ± SEM (n = 3). ***$p < 0.001$

641 (Tukey's test). *n.s.*, not significant.

642 (C) Plasma membrane integrity of cells that had been treated under the same

643 conditions as (B) was assessed by PI staining. The cells were stained with PI (red)

644 and Hoechst 33342 (blue). Bars: 100 μm.

(D) Viability of cells was assessed by CellTiter-Blue assay. Hepa 1-6 cells were treated with 10 μM erastin for 24 h in the presence or absence of NOC18 at the indicated concentrations. Data represent the mean ± SEM (n = 4). ***$p < 0.001$ (Dunnett's test, vs. erastin without NOC18). *n.s.*, not significant.

(E) Cytotoxicity of cells assessed by measuring released LDH activity. Hepa 1-6 cells were treated with 10 μM erastin for 24 h in the presence or absence of 100 μM NOC18. Data represent the mean ± SEM (n = 3). ***$p < 0.001$ (Tukey's test). *n.s.*, not significant.

(F) Plasma membrane integrity of cells that had been treated under the same conditions as (E) and assessed by PI staining. The cells were stained with PI (red) and Hoechst 33342 (blue). Bars: 100 μm.

Fig. 2. Effects of NOC18 on the intracellular status of GSH and iron during ferroptosis.

(A) Hepa 1-6 cells were incubated in conventional or cystine-free medium for 24 h in the presence or absence of 100 μM NOC18 and the intracellular contents of GSH and Cys were then measured. Data are presented as the mean ± SEM (n = 3). Different letters indicate statistically significant differences between groups ($p < 0.05$, Tukey's test).

(B) Hepa 1-6 cells were treated with 10 μM erastin for 24 h in the presence or absence of 100 μM NOC18 and the intracellular contents of GSH and Cys were then measured. Data are presented as the mean ± SEM (n = 3). Different letters indicate statistically significant differences between groups ($p < 0.05$, Tukey's test).

(C, D) Western blot analysis of GPX4 expression during ferroptosis. Hepa 1-6 cells were incubated in cystine-free medium (C) or treated with 10 μM erastin (D) for 18 h in the presence or absence of 100 μM NOC18 with β-actin as a loading control. Quantitative analysis of the protein levels of GPX4 standardized to β-actin levels

673 (Bottom). Data represent the mean ± SEM (n = 3). Different letters indicate statistically

674 significant differences between groups ($p < 0.05$, Tukey's test).

675

Fig. 3. Effects of NOC18 on the intracellular status of iron metabolism during ferroptosis.

(A) Intracellular ferrous iron assessed by flow cytometry using FerroFarRed. Hepa 1-6 cells were incubated in cystine-free medium or treated with 10 μM erastin for 18 h in the presence or absence of 100 μM NOC18. Data are presented as the mean ± SEM (n = 3). Different letters indicate statistically significant differences between groups ($p < 0.05$, Tukey's test).

(B) Hepa 1-6 cells were treated with 100 μM NOC18 for 8 h and the mRNA expression levels of *Tfrc*, *Dmt1*, *Fpn*, and *Fth1* were determined by qPCR analysis. Each value was normalized to the corresponding expression of the housekeeping gene *GAPDH*. The control NOC18-untreated cells were set to 100%. Data represent the mean ± SEM (n = 4). There were no significant differences, vs without NOC18 (Student's t-test). *n.s.*, not significant.

Fig. 4. Effects of NOC18 on lipid peroxidation during ferroptosis.

(A) Lipid peroxide production assessed by flow cytometry using C11-BODIPY$^{581/591}$. Hepa 1-6 cells were incubated in cystine-free medium or treated with 10 μM erastin for 18 h in the presence or absence of 100 μM NOC18. Data are presented as the mean ± SEM (n = 3). Different letters indicate statistically significant differences between groups ($p < 0.05$, Tukey's test).

(B) Hepa 1-6 cells were incubated in cystine-free medium or treated with 10 μM erastin for 24 h in the presence or absence of 100 μM NOC18, and then stained with anti-HNE antibodies. Bars: 100 μm.

(C) Hepa 1-6 cells were incubated in cystine-free medium or treated with 10 μM erastin for 24 h in the presence or absence of 100 μM NOC18, and then stained with FerAb antibodies. Bars: 100 μm.

703 **Fig. 5. Effects of NOC18 on ferroptosis induced by GPX4 inhibition in Hepa 1-6**
704 **cells.**

705 (A) Cytotoxicity of cells was assessed by measuring the activity of released LDH.
706 Hepa 1-6 cells were treated with 5 μM RSL3 for 24 h in the presence or absence
707 of 100 μM NOC18. Data represent the mean ± SEM (n = 3). ***$p < 0.001$
708 (Tukey's test). *n.s.*, not significant.

709 (B) Representative images of cells treated under the same conditions as in (A). Hepa
710 1-6 was stained with PI and Hoechst (Top). Alternatively, the cells were treated
711 with 5 μM RSL3 for 6 h in the presence or absence of 100 μM NOC18, and then
712 stained with FerAb antibodies (Bottom). Bars: 100 μm.

713 (C) Lipid peroxide production assessed by flow cytometry using C11-BODIPY$^{581/591}$.
714 Hepa 1-6 cells were treated with 5 μM RSL3 for 18 h in the presence or absence
715 of 100 μM NOC18. Data are presented as the mean ± SEM (n = 3). Different
716 letters indicate statistically significant differences between groups ($p < 0.05$,
717 Tukey's test).

(D) Tamoxifen-inducible GPX4 knockout Pfa1 cells were treated with 1 μM tamoxifen (Tam) for 48 h in the presence or absence of 100 μM NOC18. Western blot analysis of the expression of GPX4 during ferroptosis were then performed. β-actin was used as a loading control.

(E) Representative phase-contrast images of Pfa1 cells that had been treated under the same conditions as in (D).

(F) Cytotoxicity of cells assessed by measuring released LDH activity. Pfa1 cells were treated under the same conditions as in (D). Data represent the mean ± SEM (n = 3). ***$p < 0.001$ (Tukey's test). *n.s.*, not significant.

Fig. 6. Effects of NOC18 on TBHP-induced ferroptosis in Hepa 1-6 cells.

(A) Cytotoxicity of cells assessed by measuring released LDH activity. Hepa 1-6 cells were treated with 50 μM TBHP for 24 h in the presence or absence of 100 μM NOC18. Data represent the mean ± SEM (n = 3). ***$p < 0.001$ (Tukey's test). *n.s.*, not significant.

(B) Representative images of cells. Hepa 1-6 cells were treated under the same conditions as in (C), and assessed by PI and Hoechst staining (Top). Alternatively, cells were treated with 50 μM TBHP for 6 h in the presence or absence of 100 μM NOC18, and then stained with FerAb antibodies (Bottom). Bars: 100 μm.

(C) Cytotoxicity of cells assessed by measuring released LDH activity. Hepa 1-6 cells were treated with 50 μM TBHP for 24 h in the presence or absence of 100 μM NOC18. Data represent the mean ± SEM (n = 3). Different letters indicate statistically significant differences between groups ($p < 0.05$, Tukey's test).

Figure 1

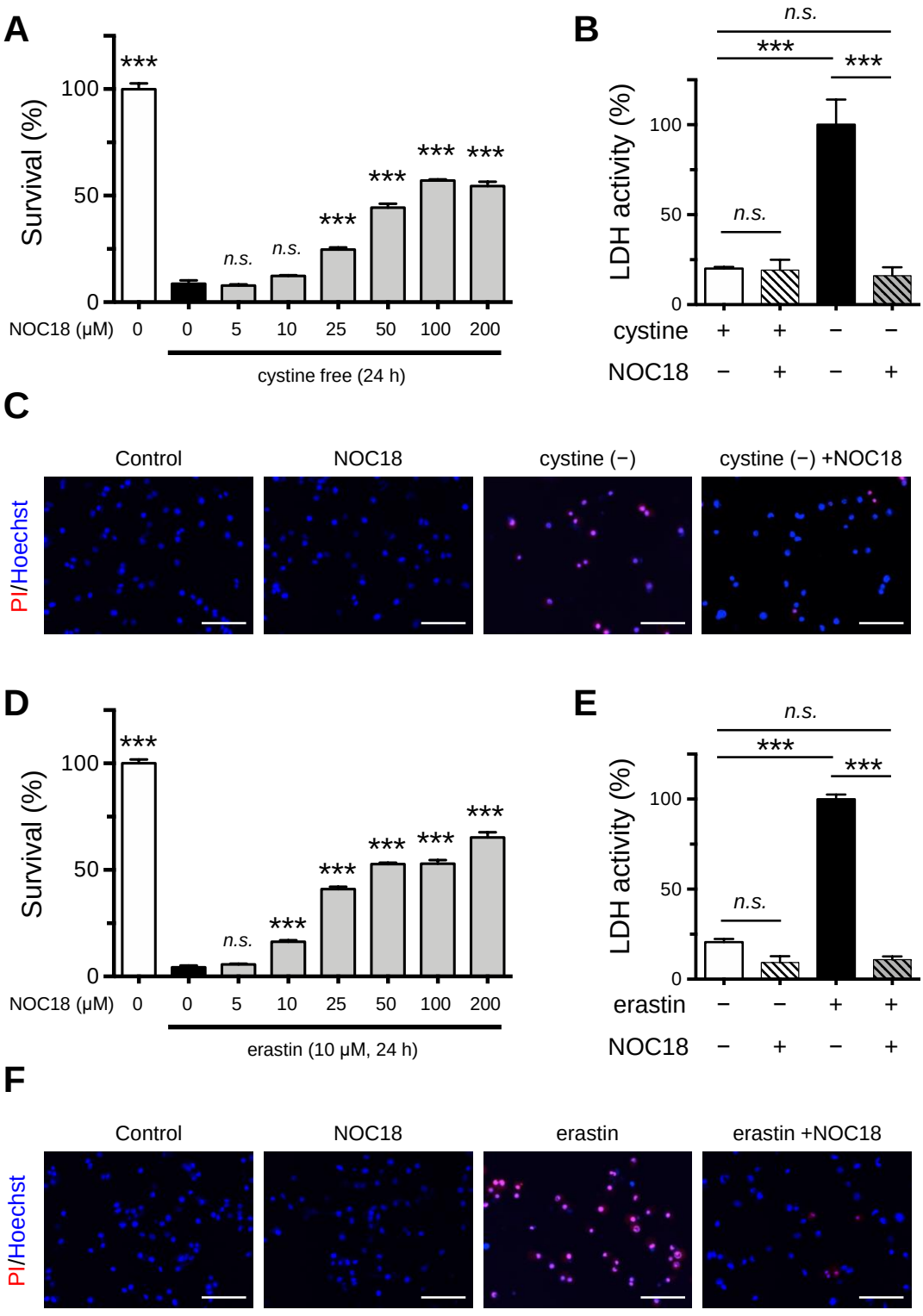
A
Survival (%)
100
50
0
***
n.s.
n.s.
***
***
***
***
NOC18 (μM) 0 0 5 10 25 50 100 200
cystine free (24 h)
B
n.s.
***
***
LDH activity (%)
100
50
0
n.s.
cystine + + − −
NOC18 − + − +
C
Control
NOC18
cystine (−)
cystine (−) +NOC18
PI/Hoechst
D
Survival (%)
100
50
0
***
n.s.
***
***
***
***
***
NOC18 (μM) 0 0 5 10 25 50 100 200
erastin (10 μM, 24 h)
E
n.s.
***
***
LDH activity (%)
100
50
0
n.s.
erastin − − + +
NOC18 − + − +
F
Control
NOC18
erastin
erastin +NOC18
PI/Hoechst

Figure 2

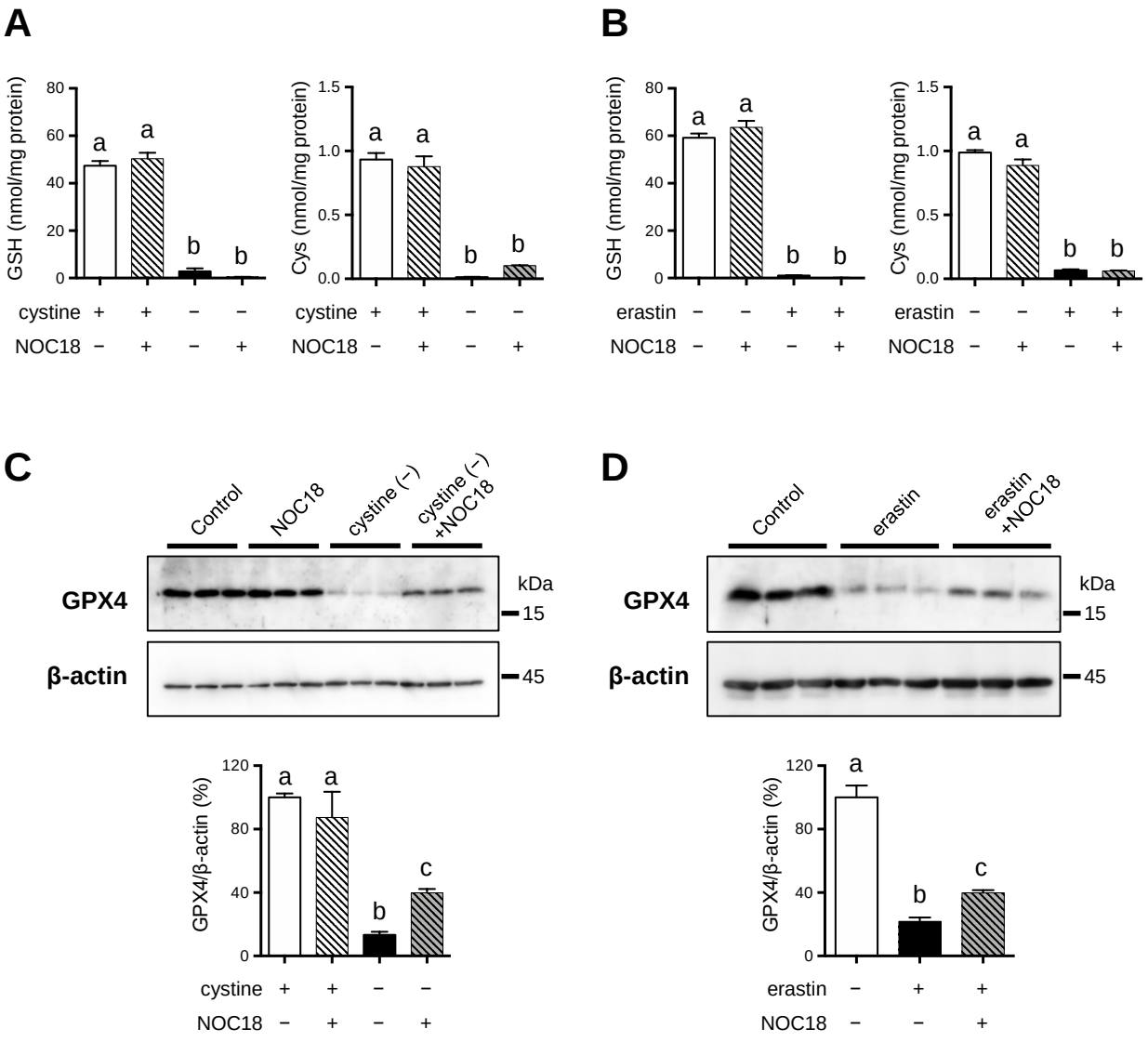
A
GSH (nmol/mg protein)
80
60
40
20
0
a
a
b
b
cystine + + − −
NOC18 − + − +
Cys (nmol/mg protein)
1.5
1.0
0.5
0.0
a
a
b
b
cystine + + − −
NOC18 − + − +
B
GSH (nmol/mg protein)
80
60
40
20
0
a
a
b
b
erastin − − + +
NOC18 − + − +
Cys (nmol/mg protein)
1.5
1.0
0.5
0.0
a
a
b
b
erastin − − + +
NOC18 − + − +
C
Control
NOC18
cystine (−)
cystine (−) +NOC18
GPX4
β-actin
kDa
15
45
GPX4/β-actin (%)
120
80
40
0
a
a
b
c
cystine + + − −
NOC18 − + − +
D
Control
erastin
erastin +NOC18
GPX4
β-actin
kDa
15
45
GPX4/β-actin (%)
120
80
40
0
a
b
c
erastin − + +
NOC18 − − +

Figure 3

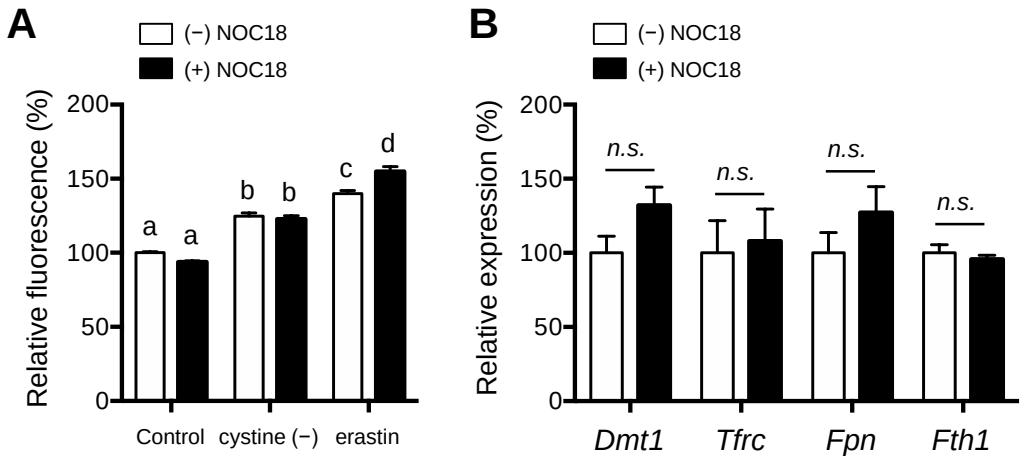
A
(−) NOC18
(+) NOC18
Relative fluorescence (%)
200
150
100
50
0
a
a
b
b
c
d
Control
cystine (−)
erastin
B
(−) NOC18
(+) NOC18
Relative expression (%)
200
150
100
50
0
n.s.
n.s.
n.s.
n.s.
Dmt1
Tfrc
Fpn
Fth1

Figure 4

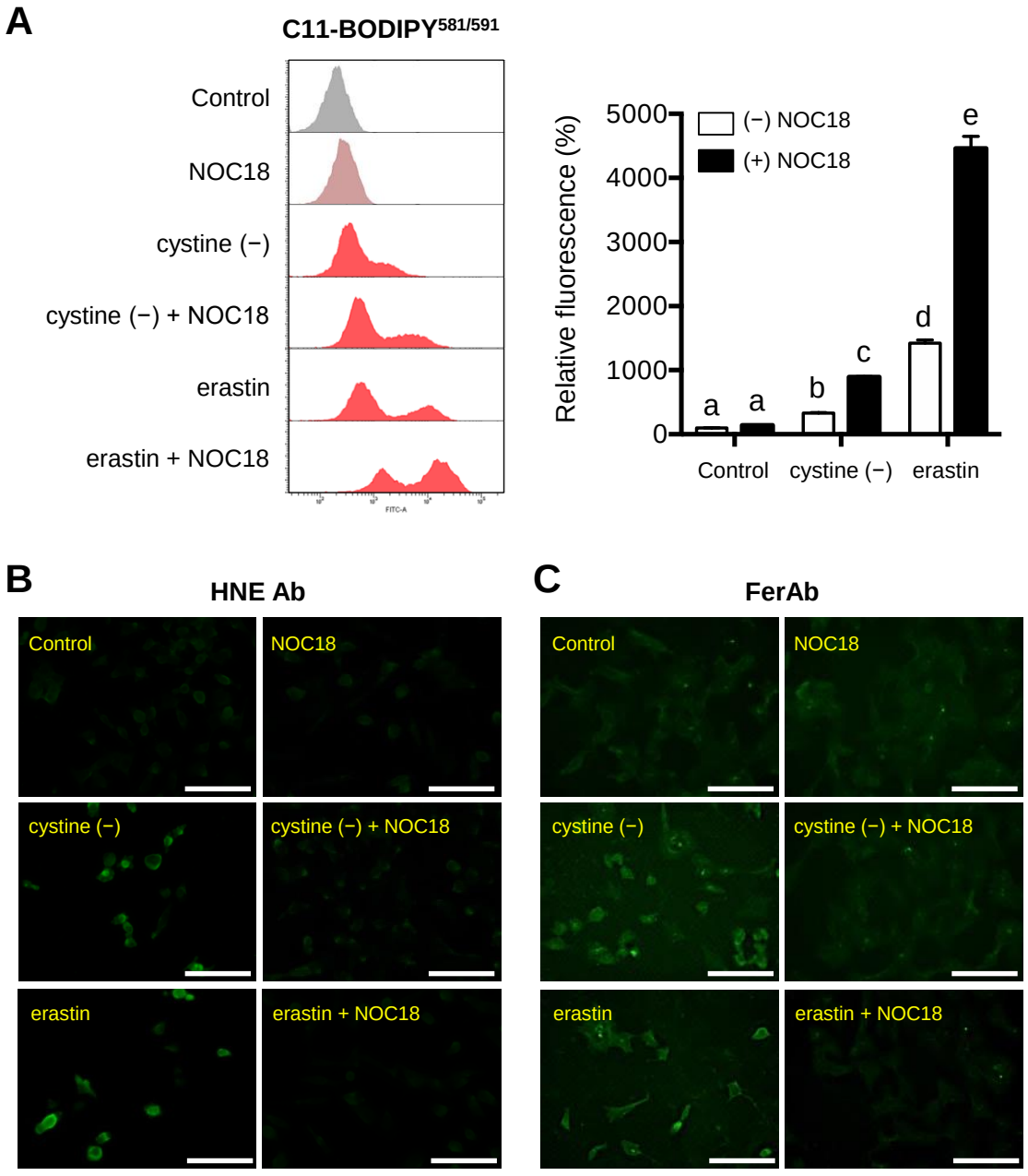
A
C11-BODIPY581/591
Control
NOC18
cystine (−)
cystine (−) + NOC18
erastin
erastin + NOC18
Relative fluorescence (%)
5000
4000
3000
2000
1000
0
(−) NOC18
(+) NOC18
a
a
b
c
d
e
Control
cystine (−)
erastin
B
HNE Ab
C
FerAb
Control
NOC18
cystine (−)
cystine (−) + NOC18
erastin
erastin + NOC18

Figure 5

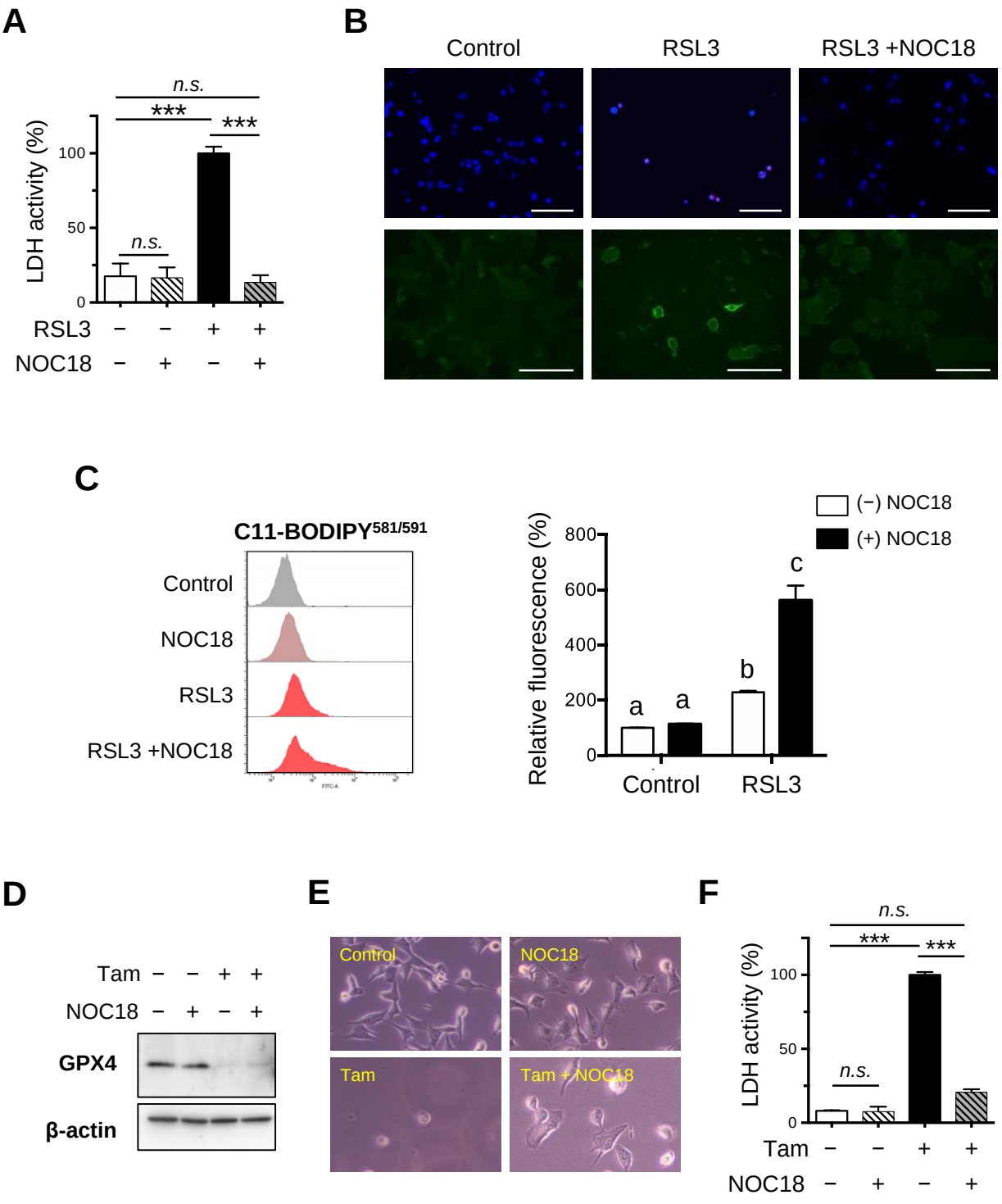
A
n.s.
***
***
LDH activity (%)
100
50
0
n.s.
RSL3 − − + +
NOC18 − + − +
B
Control
RSL3
RSL3 +NOC18
C
C11-BODIPY581/591
Control
NOC18
RSL3
RSL3 +NOC18
(−) NOC18
(+) NOC18
Relative fluorescence (%)
800
600
400
200
0
a
a
b
c
Control
RSL3
D
Tam − − + +
NOC18 − + − +
GPX4
β-actin
E
Control
NOC18
Tam
Tam + NOC18
F
n.s.
***
***
LDH activity (%)
100
50
0
n.s.
Tam − − + +
NOC18 − + − +

Figure 6

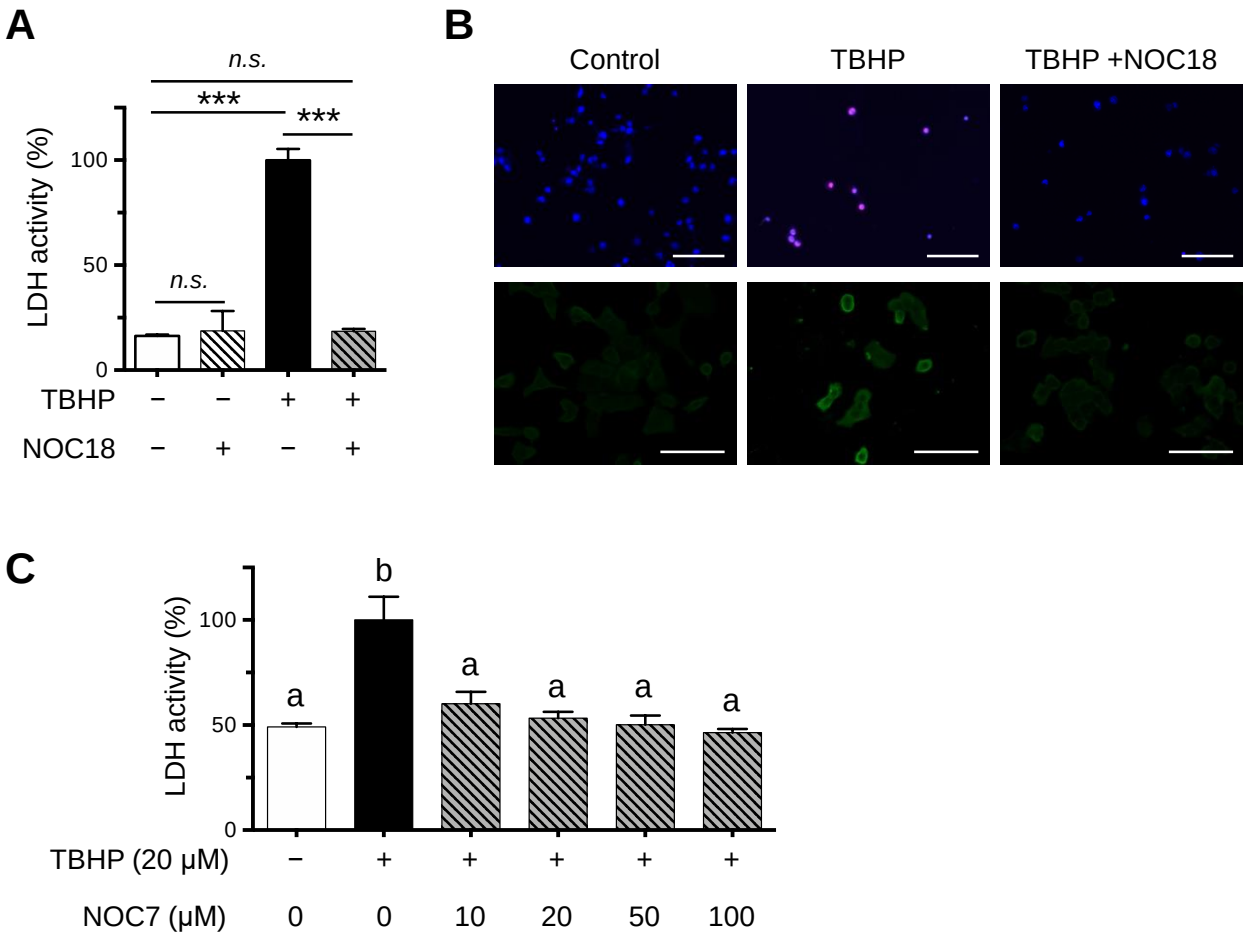
A
n.s.
***
***
n.s.
LDH activity (%)
100
50
0
TBHP − − + +
NOC18 − + − +
B
Control
TBHP
TBHP +NOC18
C
b
a
a
a
a
a
LDH activity (%)
100
50
0
TBHP (20 μM) − + + + + +
NOC7 (μM) 0 0 10 20 50 100